SHM-based fatigue damage prognostics in composite structures

L.D. Cot[1], C. Gómez[2], F. Gamboa[3], F. Kopsaftopoulos[4], F.-K. Chang[4]

[1] Institut Clément Ader, Université de Toulouse, INSA, Toulouse, FRANCE lea.cot@insa-toulouse.fr
[2] Institut National des Sciences Appliquées, Toulouse, FRANCE caegomezji@unal.edu.co
[3] Institut de Mathématiques de Toulouse, Université de Toulouse, UPS, Toulouse, FRANCE fabrice.gamboa@math.univ-toulouse.fr
[4] Structures and Composites Laboratory, Dpt Aeronautics and Astronautics, Stanford University, CA, USA fkopsaf@stanford.edu, fkchang@stanford.edu

Keywords: Parameter estimation, composite, joint extended Kalman filter, sensitivity analysis

Abstract

Our purpose addresses accurate fatigue damage prognostics in composite aircraft structures based on an SHM approach. A methodology based on the combination of an active sensing SHM technique and a state-parameter estimator to predict the fatigue damage and compute the remaining useful life of a structure is proposed. Active sensing SHM utilizes active sensors, such as piezoelectric sensors (PZTs) for monitoring local defects and can potentially interrogate large structural areas. Ultrasonic guided waves that propagate on the structure and recorded by piezoelectric sensors are used to extract damage sensitive features (damage index) for damage detection, localization and quantification. Next, the damage index and the corresponding estimated damage may be used as inputs in an appropriate fatigue model to enable the damage prognostics of the composite structure. The joint extended Kalman filter (JEKF) is used to estimate the Wu and Yao model parameters. The behavior of the JEKF is first studied by using simulated data and then experimental data. It is shown that some materials under estimation initial conditions provide better results. This combination of sensors and JEKF algorithm, teach that the real-time calculation of the remain useful life is possible and it could be sufficiently effective to be study in a real-time situation.

1. INTRODUCTION

Composite materials are emerging as the material of choice for aircraft structural components as they can improve the mechanical properties, reduce the weight, and reduce the life-cycle cost [1]. Recently, composites have been used in the aircraft fuselage of Boeing 787 and Airbus A350. Furthermore, modern aircraft are outfitted with various types of sensors and sensor networks to enable the transition from time-based to condition-based maintenance. Information processing algorithms can be integrated with sensors and signal processing to perform structural health monitoring (SHM) [2–4]. SHM has the potential to significantly reduce operational cost and maintenance related downtime.

In general, SHM technology can be classified into two types: passive and active. Passive sensing SHM utilizes continuous sensor measurements from accelerometers, strain gauges, fiber optics, etc. to monitor the structural behavior and determine the unknown global and local inputs which cause changes in sensor measurements, such as external loads, incipient damage, and temperature. On the other hand, active sensing SHM utilizes active sensors, such as piezoelectric sensors (PZTs), which can be used both as transmitters (actuators) and receivers, for monitoring local defects by generating controlled diagnostic signals into structures [5–8]. Typically, SHM methods involve the detection, monitoring, evaluation, and assessment of an adverse event that may affect the structural health state [7]. In the current state-of-the-art literature a significant amount of research is targeted to the development of diagnostic approaches based on various sensor technologies. These approaches are able to achieve a certain level of capability in terms of detection, evaluation, and assessment of adverse events that can affect the proper structural

operation, performance, and safety. However, damage prognostics and remaining useful service-life estimation remain extremely challenging tasks that necessitate the development of novel effective approaches and methodologies. In the case of active sensing SHM systems, acousto-ultrasonic guided waves are generated via the use of piezoelectric actuators and propagate on the structure. These waves are recorded by piezoelectric sensors and subsequently used for the extraction of damage sensitive features or damage indices (DIs) for damage detection, localization and quantification. Next, these damage indices and the corresponding estimated and quantified damage may be used as inputs in an appropriate prognostic model.

Our purpose addresses accurate fatigue damage prognostic based on an SHM approach. A methodology based on the combination of an active sensing SHM technique and a state-parameter estimator to predict the fatigue damage and compute the remaining useful life of a structure component is proposed. Fiber-reinforced composite materials under different fatigue loading and sequences as well as model for fatigue damage prediction proposed by Wu and Yao in [9] are considered. The fatigue phenomenological nonlinear model depending on two uncertain material parameters is derived from stiffness degradation rule and was verified with experimental data. A sensitivity analysis has been performed based on the methodology proposed by Lemaître et al. [10]. In order to get accurate values, the two model parameters are estimated using the joint extended Kalman filter (JEKF) method. Indeed, the EKF method based on a recursive digital processing is appropriate to real time applications such as active sensing SHM method. First, simulated data generated from the Wu and Yao model are used to estimate the two parameters. Glass fiber and carbon fiber composite materials under various fatigue loading have been tested. The influence of the process and measurement noises has been studied. The impact of parameter initial values and of the DI and parameter variances on the estimation have been also studied. Materials tested show a similar general trend. But estimation error magnitudes on DI's and parameters depend on material. Moreover, a better error estimation is always obtained when the process noise is smaller than the measurement noise. Fatigue damage expermiemental data are processed to JEKF state-parameter estimation.

2. ACTIVE SENSING SHM SYSTEM

When an elastic wave travels through a region where there is a change in material properties, scattering occurs in all directions. Active sensing methods utilize the distributed actuator/sensors, permanently attached to the structure, to generate the elastic wave and measure the arriving waves at sensors [6]. The damage diagnosis is performed through the examination of the arriving waves including the scattered wave in comparison with a "baseline" condition. When a single actuator–sensor path is considered for damage interrogation, the amount a signal changes is quantified as scattered energy and may be related to the change in local material properties. Since the scattered energy contains the information of both attenuation and phase delay of the directly transmitted wave due to the presence of a flaw, an appropriate damage index can be selected to correlate the change in sensor measurements to crack size.

Typically, SHM involves four functional levels referred to as Technology Classification Levels (TCL) [7]: (i) damage detection, (ii) identification/localization, (iii) quantification, and (iv) estimation of the remaining service life/strength (prognosis). The performance of an active sensing SHM system depends upon several key parameters, such as the type, number and location of sensors, the inspection interval, and the diagnostic algorithms used to process and interpret the sensing data [7]. A schematic representation of an active sensing SHM system is presented in Figure 1.

In active sensing SHM systems, acousto-ultrasonic guided waves are generated via the use of piezoelectric actuators, that can also operate as sensors, and propagate on the structure. Typically, sensor data may be collected either over predetermined time intervals in a scheduled manner or continuously in an automatic way. In that respect, the effectiveness of an SHM system is affected by the sensor/actuator network (number and locations of sensors and actuators). Next, the ultrasonic signals are recorded by the available piezoelectric sensors (see Figure 1). Each sensor-actuator pair forms a distinct signal propagation path with an appropriate number of paths to be determined based on the employed diagnostic

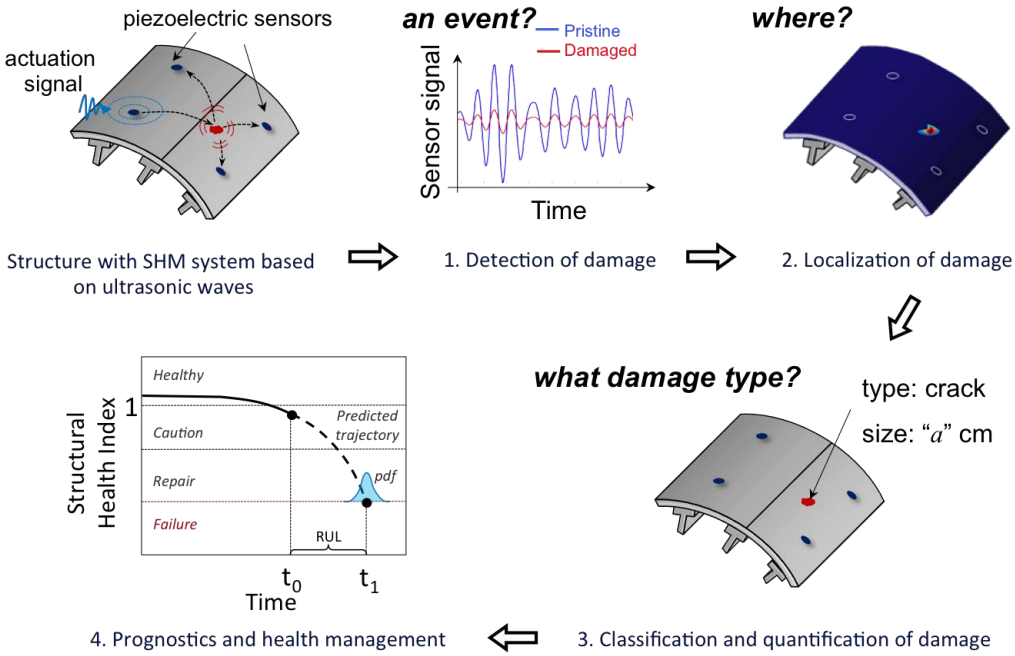

Figure 1: Schematic representation of the generic active sensing SHM principles of operation [7].

approach. In general, the use of more sensors and corresponding paths may increase the accuracy of the diagnostic algorithm [7, 8]. Using the available ultrasonic signals and appropriate signal processing techniques damage sensitive features, usually referred as damage index (DI), are extracted under various operating conditions (temperature, loads, etc.) during the service life of the structure. These DIs are subsequently utilized for tackling the tasks of damage detection, damage localization, and damage quantification. The extracted DIs along with the information related to the damage location and damage size (e.g. crack length, matrix crack density for composites, delamination area, etc.) can be used in the prognostic model building stage for the estimation of the remaining strenght/useful life and the determination of appropriate maintenance and life-cycle management approaches. In this preliminary study, the Wu and Yao [9] model, that takes into account the damage growth at different fatigue loading levels is considered.

The diagnostic effectiveness characterization of SHM systems requires understanding of the way the various system parameters affect the sensor signals. Once the effects are understood and properly quantified, it is crucial to select a damage index that is insensitive to all other environmental and external factors other than damage. The DI that is highly sensitive to damage and much less sensitive to other external factors will be selected for detecting, localizing, and characterizing the damage presence on the structure. Therefore, the diagnostic sensitivity of the SHM system depends highly on the appropriate selection of the DI. In a recent study [7], it was proved that the DI formulation may solely depend on the coefficients related to the guided wave propagation.

3. SENSITIVITY ANALYSIS DAMAGE MODEL

For our study, the recent phenomenological damage growth model for composites proposed by Wu and Yao [9] is used. The material stiffness degradation is used as the damage evolution parameter. The Wu and Yao model uses extensive experimental data to determine the empirical parameters and gives results for E-glass/epoxy and Carbon/epoxy models. Generally, a large amount of experimental data leads to a better fitting damage growth model. Wu and Yao describes the whole fatigue life evolution of composite

materials as

$$D(n) = 1 - \left(1 - \left(\frac{n}{n_l}\right)^B\right)^A \tag{1}$$

where D is the normalized accumulated damage at loading cycle n depending on material property parameters A and B, and n_l is the fatigue life at the corresponding applied load level.

A sensitivity analysis of parameters A and B on structure component probability of failure is addressed by considering the perturbation methodology proposed by Lemaître et al. [10]. Sensitivity indices allow us to quantify the impact of input random variables such as parameters A and B on the probability of failure. The main idea is to modify the probability density function of input random variables, for instance, by a mean shifting of these random variables and analyze the consequence on the probability of failure. In this case, the mean of a random variable X is a perturbation δ instead of the expectation $\mathbb{E}[X]$ of the distribution with no perturbation. The perturbed probability of failure is therefore computed. The perturbation δ is $\mu + \delta\sigma$ where $\mu = \mathbb{E}[X]$ and σ is the standard deviation of the distribution with no perturbation.

The crude Monte Carlo method is carried out to provide a statistical estimation $\hat{P}_f$ of the probability of failure

$$\hat{P}_f = \frac{1}{N}\sum_{i=1}^{N} \mathbb{1}_{G(x_i,t)>y_{th}}(x_i) \tag{2}$$

where $Y = G(X,t)$ is a deterministic model depending on an input random variable $X \in \mathbb{R}^m$ of known density f, $t \in \mathbb{R}^p$ is an input deterministic variable and $Y \in \mathbb{R}$ is an output random variable. N is the sample size. In the context of structural monitoring, a structure component is failed if the value of the scalar y returned by function G is greater than a predefined threshold y_{th}. A failure criterion is therefore defines as $y = G(x,t) > y_{th}$ where x is a realization of vector X.

In (2), it is assumed that $X_i \sim X$ and the uncertainty on the estimation of $\hat{P}_f$ is $Var(\hat{P}_f) = \frac{\hat{P}_f(1-\hat{P}_f)}{N}$. The Wu and Yao model is used to compute the damage growth at a certain number of cycles. According to Eq. 1,

$$G(X,t) = 1 - (1 - t^B)^A \tag{3}$$

where $t = \frac{n}{n_l} \in \mathbb{R}$ and $X = (A,B)^T \in \mathbb{R}^2$ where A and B are input random variables associated to model uncertain parameters A and B. These random variables are sampled from their distributions assuming that that they follow a normal distribution with parameter values as means and standard deviations of 5% from Table 1 in [9]. Sensitivity analysis is performed for the glass fiber material defined at the first line of this table. In a first approximation, one assumes that variables A and B are not correlated. A structure made with 500 identical structure components is considered. For all calculations, the Monte Carlo sample drawn is 1000 and the failure threshold value is 0.6. Sensitivity indices are computed at predetermined loading cycle numbers. Figures 2 and 3 show estimated indices for the Monte Carlo model with a mean shifting at loading cycles 48000. At a number of cycles of 36000, the Monte Carlo simulation based on a size sample of 500000 provides an estimated failure probability of 210^{-6}, means only one structure component failed. In this case, the variance of the sensitivity indices is not possible.

At 48000 cycles, the estimated failure probability is 3.3510^{-3}, means 1675 structure components failed. Figure 2 shows the impact of parameter A on the failure probability. An increase of the parameter A mean raises the failure probability. For $\delta = 1$, the new failure probability is 10 times larger than the one with the unperturbed distribution. A decrease of A mean diminishes the failure probability. For $\delta = -0.7$, the failure probability is divided by 10 than the one with the unperturbed distribution. Figure 3 shows the impact of parameter B on the failure probability. The magnitude is lesser than parameter A one and the impact of B is opposite to A one. This means that an increase of B leads to a decrease of the failure probability with a factor 20 and inversely. Parameter B has a low impact on the failure probability.

At 56000 cycles, the estimated failure probability is 2.28810^{-3}, means 114385 structure components failed. It is observed that parameter B has a low impact increasing with a mean decrease and inversely.

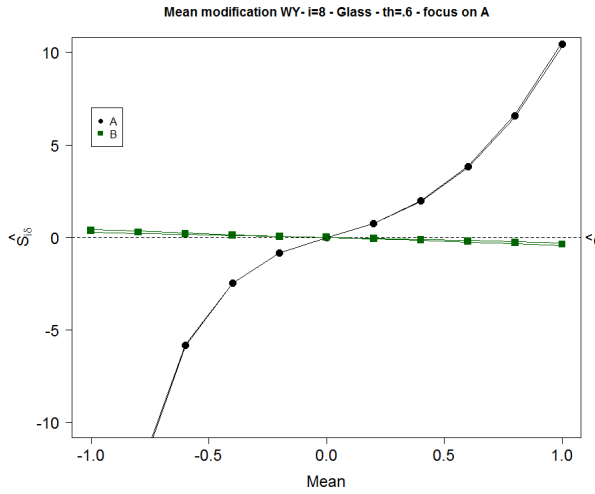

Figure 2: Parameter A for glass fiber FRC_{glass}.

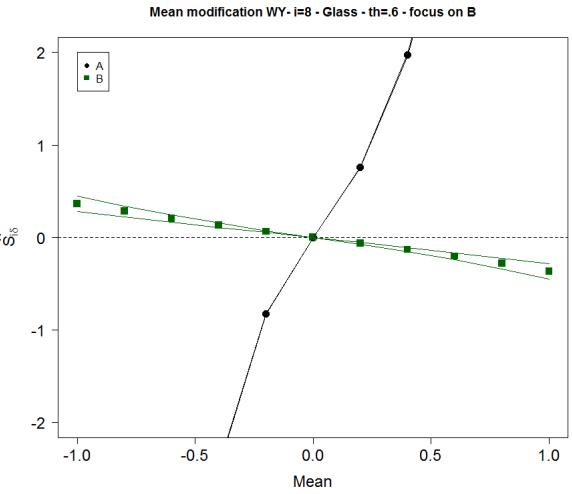

Figure 3: Parameter B for glass fiber FRC_{glass}.

Parameter A has a strong impact. The failure probability is doubled for $\delta = 1$ and it is divided by 5 for $\delta = -1$. Sensitivity analysis shows that, in a first approximation, parameter A appears to be more influent on the failure probability of a glass fiber composite structure component than parameter B. It is therefore important to get a good estimation of parameter A.

4. STATE-PARAMETER ESTIMATION MODELLING

In this section, the estimation problem modelling based on the JEKF is described. First, the JEKF method is briefly introduced; then, it is applied to the Wu and Yao parameter model estimation.

4.1 Joint extended Kalman filter method

The JEKF method consists in the use of the augmented state vector $X_k \in \mathbb{R}^{n+q}$ at time $k \in \mathbb{N}$ defined as $X_k = (S_k, \Lambda_k)^T$ where $S_k \in \mathbb{R}^n$ represents the random vector of the system state and $\Lambda_k \in \mathbb{R}^q$ the unknown vector of parameters. The modelling of a nonlinear discrete dynamical system based on the joint formulation lead to the equations

$$\left\{ \begin{array}{lcll} S_k & = & f(S_{k-1}, \Lambda_{k-1}, k-1) + C_{k-1} W_{k-1} & \textit{Dynamics} \\ \Lambda_k & = & id(\Lambda_{k-1}) + Y_{k-1} & \textit{Parameter} \\ Z_k & = & h(S_k, k) + V_k & \textit{Observation} \end{array} \right. \tag{4}$$

Nonlinear functions f and h are defined on $\mathbb{R}^n$ and take their values in $\mathbb{R}^n$ et $\mathbb{R}^p$ respectively. They represent the state process and measurement evolution. The second equation means that parameters do not evolve over time. In the third equation, $Z_k \in \mathbb{R}^p$ is the random observation vector at time k (output). $\{W_k\} \in \mathbb{R}^m$, $\{Y_k\} \in \mathbb{R}^q$ and $\{V_k\} \in \mathbb{R}^p$ are series of random vectors representing the state (or process) noise, parameter noise and observation noise. $C_k \in \mathscr{M}_{n,m}(\mathbb{R})$ is the deterministic matrix of state noise. The Jacobian matrix $J_k(\hat{X}_{k-1})$ at time k relative to the augmented state X_k evaluated at the last estimate $\hat{X}_{k-1} = (\hat{S}_{k-1}, \hat{\Lambda}_{k-1})^T$, i.e. at time $k-1$, is

$$J_k(\hat{X}_{k-1}) = \begin{pmatrix} J_{f,k}(\hat{S}_{k-1}) & J_{f,k}(\hat{\Lambda}_{k-1}) \\ J_{id,k}(\hat{S}_{k-1}) & J_{id,k}(\hat{\Lambda}_{k-1}) \end{pmatrix}$$

where $J_{f,k} \in \mathscr{M}_n(\mathbb{R})$ is the Jacobian matrix of f with respect to S, $J_{f,k}(\hat{\Lambda}_{k-1}) \in \mathscr{M}_{n,q}(\mathbb{R})$ is the Jacobian matrix of f with respect to Λ, $J_{id,k} \in \mathscr{M}_{q,n}(\mathbb{R})$ is the Jacobian matrix of the identity function with respect to S and $J_{id,k}(\hat{\Lambda}_{k-1}) \in \mathscr{M}_q(\mathbb{R})$ is the Jacobian matrix of the identity function with respect to Λ.

Observing that $J_{id,k}(\hat{S}_{k-1}) = 0_{q,n}$ and $J_{id,k}(\hat{\Lambda}_{k-1}) = I_q$, therefore

$$J_k(\hat{X}_{k-1}) = \begin{pmatrix} J_{f,k}(\hat{S}_{k-1}) & J_{f,k}(\hat{\Lambda}_{k-1}) \\ 0_{q,n} & I_q \end{pmatrix} \tag{5}$$

where $J_{f,k}(\hat{S}_{k-1}) = \frac{\partial f^{(i)}(S,\Lambda)}{\partial s^{(j)}}\Big|_{(S=\hat{S}_{k-1},\Lambda=\hat{\Lambda}_{k-1})}, \ \forall 1 \leq i,j \leq n,$

and $J_{f,k}(\hat{\Lambda}_{k-1}) = \frac{\partial f^{(i)}(S,\Lambda)}{\partial \lambda^{(j)}}\Big|_{(S=\hat{S}_{k-1},\Lambda=\hat{\Lambda}_{k-1})}, \ \forall 1 \leq i \leq q, \ 1 \leq j \leq n.$

According to the observation equation from system (4) the Jacobian matrix of h evaluated at the state prediction $\hat{X}_k^-$ at time k is

$$H_k = \frac{\partial h^{(i)}(S,k)}{\partial x^{(j)}}\Big|_{X=\hat{X}_k^-}, \ \forall 1 \leq i,j \leq p.$$

The standard algorithm for the EKF method is then applied to solve system (4).

Algorithm 1 Joint EKF algorithm

Initialization: $\hat{X}_0^-, P_0^-, \hat{\Lambda}_0^-$

Prediction:
$$\begin{cases} \hat{X}_k^- &= f(\hat{X}_{k-1}) \\ P_k^- &= J_k(\hat{X}_{k-1})P_{k-1}J_k(\hat{X}_{k-1})^T + C_{k-1}Q_{k-1}C_{k-1}^T \end{cases}$$

Correction:
$$\begin{cases} K_k &= P_k^- H_k^T (H_k P_k^- H_k^T + R_k)^{-1} \\ \hat{X}_k &= \hat{X}_k^- + K_k(Z_k - h(\hat{X}_k^-)) \\ P_k &= (I_n - K_k H_k)P_k^-. \end{cases}$$

Output: State-parameter estimation $\hat{X} = \hat{X}_k$ and covariance matrix estimation error $P = P_k$

4.2 Application to the Wu and Yao model

The JEKF method is now applied to estimate the fatigue index damage D and parameters A and B of Eq. 1. In this case, the joint vector is $X = (D,A,B)^T$. Assuming that $Y = O_q$, system (4) become

$$\begin{cases} D_k &= f(D_{k-1},\Lambda_{k-1}) + C_{k-1}W_{k-1} \\ \Lambda_k &= id(\Lambda_{k-1}) \\ Z_k &= HD_k + V_k \end{cases} \tag{6}$$

where the vector to be estimated is $\Lambda = (A,B)^T$ and the sensitivity matrix is $H = (100)$ because only DI is observed. The first recurrent equation in (6) is obtained by approximating the first derivative expressing the rate of DI (7) by a finite difference. From

$$D'(n) = \frac{A\,B}{n_l}\left(\frac{n}{n_l}\right)^{B-1}\left(1 - \left(\frac{n}{n_l}\right)^{B}\right)^{A-1} \tag{7}$$

we obtain $D_k = f(D_{k-1},\Lambda_{k-1})$ where function f is defined as

$$f(D_{k-1},\Lambda_{k-1}) = D_{k-1} + \frac{A\,B}{n_l}\left(\frac{n_{k-1}}{n_l}\right)^{B-1}\left(1 - \left(\frac{n_{k-1}}{n_l}\right)^{B}\right)^{A-1}(n_k - n_{k-1}). \tag{8}$$

The JEKF requires the computation of the Jacobian matrix $J_k(\hat{X}_k)$ at step k defined in (5). This matrix is expressed as

$$J_k(\hat{X}_k) = \begin{pmatrix} J_{f,k}(\hat{D}_{k-1}) & J_{f,k}(\hat{A}_{k-1}) & J_{f,k}(\hat{B}_{k-1}) \\ 0 & 1 & 0 \\ 0 & 0 & 1 \end{pmatrix} \tag{9}$$

where $J_{f,k}(\hat{D}_{k-1}) = \frac{\partial f(D,\Lambda)}{\partial D}\Big|_{(D=\hat{D}_{k-1},\Lambda=\hat{\Lambda}_{k-1})}$, $J_{f,k}(\hat{A}_{k-1}) = \frac{\partial f(D,\Lambda)}{\partial A}\Big|_{(D=\hat{D}_{k-1},\Lambda=\hat{\Lambda}_{k-1})}$ and $J_{f,k}(\hat{B}_{k-1}) = \frac{\partial f(D,\Lambda)}{\partial B}\Big|_{(D=\hat{D}_{k-1},\Lambda=\hat{\Lambda}_{k-1})}$.

5. RESULTS AND DISCUSSION

5.1 Methodology

Both DI D and parameters A and B are estimated using the JEKF. A first step consists in the study of the JEKF behavior by using DI simulated data generated from Eq.1 and adding a Gaussian noise. Three glass fiber and carbon fiber composite materials under various fatigue loading addressed in Table 1, [9], have been tested. Then, for the thirteen materials mentioned in this table, experimental data are used to perform the state-parameter estimation.
As said, the first study is based on DI data generation using the Wu and Yao model with parameter values of A and B provided in Table 1, measurement time interval is every 100 cycles and whole fatigue life is $n_l = 10000$ cycles. The additive noise is a normal distribution with mean zero and standard deviation of 5%. Three different composite materials have been considered:

- the glass fiber HC9106-3 $[0/90_3]$, called FRC_{glass}, under a fatigue loading level of 75% of its ultimate strength σ_{ult} whose corresponding parameter values $A = 0.314$ and $B = 0.025$,
- two carbon fiber composites T300/QY8911 with sequences $[45/90/-45/0_2/-45/90/45]$ and $[0_2/45/0_2/-45/0/90]$, called FRC_a and FRC_c, under fatigue loading levels of 441.7 MPa and 917.5 MPa, whose corresponding parameter values $A = 0.703$, $B = 0.445$ and $A = 0.571$, $B = 0.057$ respectively.

The framework proposed in this paper is first validated by taking into account parameter values of Table 1, [9], to generate data and to initialize the JEKF process. A reference case is therefore obtained. Then a deep sensitivity analyzis is carried out by studying the impact of the JEKF inputs on estimation results. First, the impact of process and noise covariance matrices Q and R on the estimation is studied. Three cases are considered: $R > Q$, $R = Q$ and $R < Q$ as mentioned in Table 1 below, which shows the JEKF input values successively used to estimation process. In a second step, for each one of these three cases,

Estimation initial conditions	
Process and measurement noises	R >Q: $R = 0.1$, $Q = 0.001$
	R = Q: $R = 0.01$, $Q = 0.01$
	R <Q: $R = 0.001$, $Q = 0.1$
P_{0D}	0.1 - 0.01 - 0.001 - 0.0001
P_{0A}	0.01 - 0.001 - 0.0001 - 0.00001
P_{0B}	1 - 0.1 - 0.01 - 0.001 - 0.0001
Initial prediction error	1%, 10% and 20%

Table 1: JEKF algorithm inputs.

the influence on the estimation of initial variances P_{0D}, P_{0A}, P_{0B}, i.e. initial diagonal coefficients of matrix P, on variables D, A and B respectively is successively studied. This means that P_{0A} and P_{0B} are set, and P_{0D} varies with values given in Table 1. Estimation error evolution (EEE) on D, A and B is then plot and analyzed. In the same way, P_{0D} and P_{0A} are set, P_0B varies and the EEE on D, A and B is analyzed. Finally, the role of P_{0A} and P_{0B} is inverted and the EEE on D, A and B is addressed. A third step consists in analyzing the impact of the initial joint vector prediction $\hat{X}_0^- = (\hat{D}_0^-, \hat{A}_0^-, \hat{B}_0^-)^T$ by assuming that this vector is known with an error of 1%, 10% or 20%. For each one of these error values, the variation of initial variances on D, A and B is combined and a similar study as previously is realized. This third step is repeated for each three cases $R > Q$, $R = Q$ and $R < Q$.

The second study consists in performing state-parameter estimation based on real data from fatigue experiment on thirteen composite fibers provided in [9] - see Table 1 and Fig. 2. For each material, systematic simulations have been done by gradually modifying the JEKF input values, means initial variances P_{0D}, P_{0A} and P_{0B}, measurement noise R and process noises Q_D, Q_A, Q_B on D, A and B respectively, in order to find the better JEKF initial variable values leading to an acceptable estimation of D, A and B. All these values are between 10^{-5} and 10^{2}. At each simulation, only one variable value is changed by increasing its exponent of one. Each variable has therefore 8 different values. $8^7 = 2097152$ simulations have been performed. For the 13 materials, the better trade-off between the seven input variables leading to the smaller relative state-parameter estimation error is kept for other simulations.

5.2 Estimation from simulated data

5.2.1 Process and measurement noise sensitivity

In the case $R < Q$, the EEE on D, A and B are same for all simulations with both glass and carbon fibers. In the case $R = Q$, the EEE are same for all simulations with carbon fibers and same or very close for glass fiber. In the case $R > Q$, variations are observed with different evolutions depending on materials. For carbon fibers, the EEE is same or very close when either the variance on D varies, either the variance on B varies. But when the variance on A varies, larger variations are observed on the EEE on A. For glass fiber, except for the reference case, larger variations are observed on the EEE on D, A and B.
From EEE numerical value point of view, estimation error obtained with carbon fibers are greater than those obtained with glass fibers. Values will be given in the next section. But we observe that, for all materials, a better error estimation is always obtained with a process noise Q smaller than a measurement noise R.

5.2.2 Initial variances and joint vector sensitivity

Sensitivity to both initial variances P_{0D}, P_{0A}, P_{0B} and initial joint vector prediction $\hat{X}_0^-$ is studied according to the framework described in 5.1. For carbon fiber FRC_a in cases $R = Q$ and $R < Q$, the EEE curves show similar trends for any variance values and are counfounded. It is also noted that the estimation error on A and B increases and oscillates with cycles, with a larger amplitude for B. For $R > Q$, in the case where D varies, EEE curves on D, A and B have a same trend, very close at the begining of the iterative process to finally merge. In case where variance on A changes, for initial prediction errors of 10% and 20%, the greater the variance is, the smaller the EEE on A is while it is the contrary in the reference case. So, the effect of a large variance on A is compensated by a large initial prediction error. No variation is observed on the EEE on B. When variance on B changes, the greater the variance is, the greater the EEE is with little difference between EEE curves. Regarding the EEE on A, the estimation error increases with cycles when variance on B increases; but, as above, this effect is compensated by a greater initial prediction error. Moreover, the impact on A is greater than the one on B. The EEE on B has a similar trend than previous cases, i.e. $R = Q$ and $R < Q$ but the EEE on A is very different. Fig. 4 highligths sensitivity of parameters A and B on estimations.
Still for FRC_a, estimation errors on D are less than 0.04 if $R > Q$, 0.1 if $R = Q$ and 0.14 if $R < Q$. The maximum estimation error on A, in the case of a 20% error on the prediction, is around 0.16 if $R > Q$, 0.24 if $R = Q$ and 0.35 if $R < Q$. The maximum estimation error on B, in the case of a 20% error on the prediction, is around 0.1 if $R > Q$, 0.14 if $R = Q$ and 0.18 if $R < Q$. Same order of magnitude is observed for FRC_c material. For $R > Q$, A also shows larger variation than B and is more influent. However, the EEE increase with variance on A is not compensated by a high initial prediction error.
For glass fiber FRC_{glass}, in the case $R < Q$, there is no impact of initial variances. In the case $R = Q$, either EEE curves are merged either they differ with very small discrepancies. In case $R > Q$, similar analysis is done as in the case of FRC_a material. Moreover, for FRC_{glass}, estimation errors on D are less than 0.1 in the 3 cases $R > Q$, $R = Q$, $R < Q$. The maximum estimation error on A, in the case of a 20%

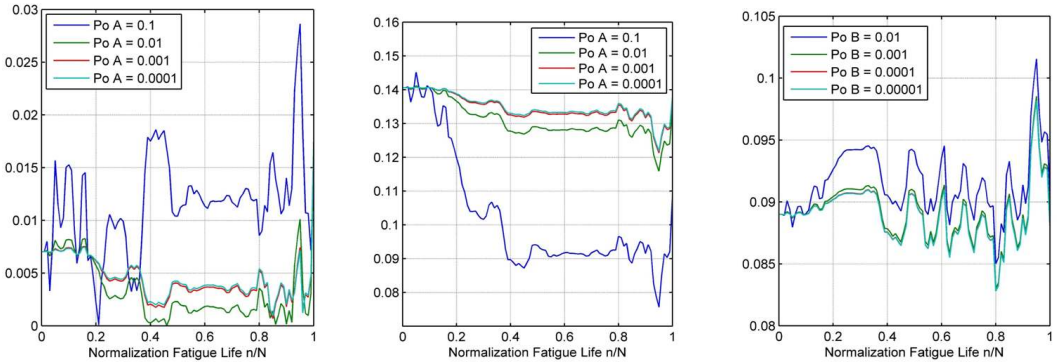

Figure 4: Estimation error for FRC_a in the case $R > Q$ - Left: Parameter A , initial prediction error 1%, Center: Parameter A, initial prediction error 20%, Rigth: Parameter B, initial prediction error 20%.

error on the prediction, is around 0.07 if $R > Q$, 0.2 if $R = Q$ and 0.9 if $R < Q$. The maximum estimation error on B, in the case of a 20% error on the prediction, is around 0.045 if $R > Q$, 0.18 if $R = Q$ and 0.35 if $R < Q$. Fig. 5 refers to these results.

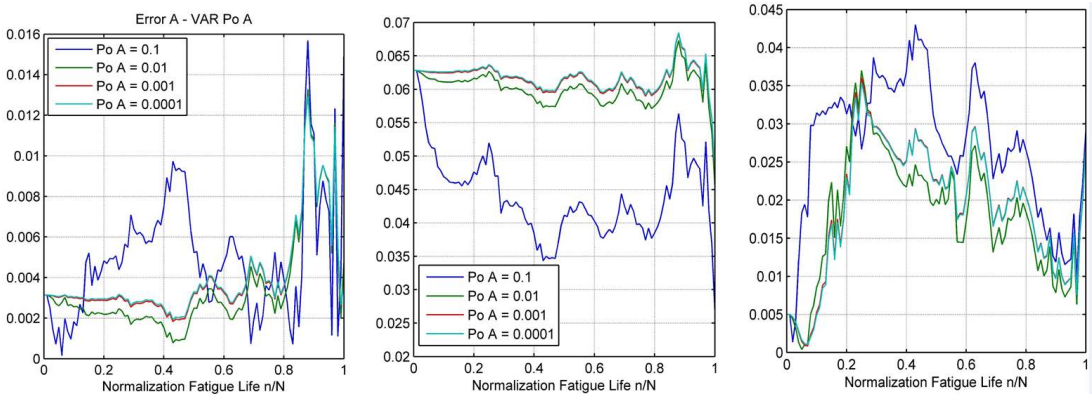

Figure 5: Estimation error for FRC_{glass} in the case $R > Q$ - Left: Parameter A , initial prediction error 1%, Center: Parameter A, initial prediction error 20%, Rigth: Parameter B, initial prediction error 20%.

In conclusion, each simulation lead to a different JEKF behavior that depends on material considered. But, similarities on the EEE on A and B, in cases $R = Q$ and $R < Q$, for both FRC_a and FRC_{glass} are noted. In the case $R > Q$, parameter A shows large variations for the three materials while variations of parameter B are smaller. This means that parameter A has more influence on the estimation than parameter B. These results are in accordance with theoretical sensitivity results mentioned in section 3.

5.3 Estimation from real data

Results obtained with fatigue DI real data are now presented. As explained in section 5.1, a systematic process allows to select materials leading to acceptable state-parameter estimations on both D, A and B. Only two materials, FRC_{glass} and the unaged specimen AS4/PR500 $[0/90_{w2}]$, called UAS, are candidates. For FRC_{glass}, only six measurements in its whole life are avalaible. Nevertheless, the JEKF works and provides an estimation on A between 0.300 and 0.315 and an estimation of B close to 0.025. Fig. 6 shows parameter estimation for UAS material where estimations are represented by little triangles. Even if there are only few DI real data, the JEKF provides a good estimation of parameters A and B close to experimental parameter values $A = 0.715$ and $B = 0.475$ (see [9]).

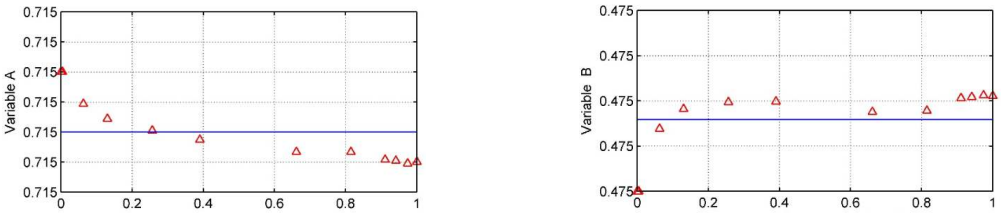

Figure 6: JEKF estimation from real data for UAS material.

6. CONCLUSION

In this paper, a framework based on the combination of an active sensing SHM technique and a state-parameter estimator allowing to obtain accurate fatigue model parameter values for composite material is proposed. Fatigue damage can therefore be predicted and remaining useful life of structure components computed. A theoretical sensitivity analysis shows that parameter B has less influence on the failure probability of a glass fiber composite structure component than parameter A. A good estimation of parameter A is therefore useful. Estimations of A and B performed using JEKF with simulated data for glass fiber and carbon fiber composite materials under various fatigue loading show that, for all materials, a better error estimation is obtained with a process noise Q smaller than a measurement noise R. Moreover, in this case, parameter A shows larger variations than parameter B and has more influence on the estimation than parameter B. These results are in accordance with theoretical sensitivity analysis. Finally, based on fatigue DI real data, the JEKF provides a good estimation of parameters A and B close to experimental parameter values corresponding to the composite material tested.

REFERENCES

[1] C. Soutis. Fibre reinforced composites in aircraft construction. *Progress in Aerospace Sciences*, 41(2):143–151, 2005.

[2] C. Boller and N. Meyendorf. State-of-the-art in structural health monitoring for aeronautics. In *Proc. of Internat. Symposium on NDT in Aerospace*, 2008.

[3] C. Boller, F.-K. Chang, and Y. Fujino. *Encyclopedia of structural health monitoring*. John Wiley, 2009.

[4] C. Boller and M. Buderath. Fatigue in aerostructures where structural health monitoring can contribute to a complex subject. *Philosophical Transactions of the Royal Society of London A: Mathematical, Physical and Engineering Sciences*, 365(1851):561–587, 2007.

[5] G. Park, C. R. Farrar, F. Lanza Di Scalea, and S. Coccia. Performance assessment and validation of piezoelectric active-sensors in structural health monitoring. *Smart Materials and Structures*, 15(6):1673–1683, 2006.

[6] J.-B. Ihn and F.-K. Chang. Pitch-catch Active Sensing Methods in Structural Health Monitoring for Aircraft Structures. *Structural Health Monitoring*, 7(1):5–19, 2008.

[7] V. Janapati, F. Kopsaftopoulos, F. Li, S.J. Lee, and F.-K. Chang. Damage detection sensitivity characterization of acousto-ultrasound-based structural health monitoring techniques. *Structural Health Monitoring*, 15(2):143–161, 2016.

[8] V. Janapati, F. P. Kopsaftopoulos, S. Roy, I. Mueller, S. J. Lee, P. Ladpli, and F.-K. Chang. Sensor Network Configuration Effect on Detection Sensitivity of an Acousto-Ultrasound- based Active SHM System. In F.-K. Chang, editor, *Proceedings of the 9th International Workshop on Structural Health Monitoring (IWSHM)*, Stanford, CA, USA, 2013. DEStech Publications, Inc.

[9] F. Wu and W. Yao. A fatigue damage model of composite materials. *International Journal of Fatigue*, 32(1):134–138, 2010.

[10] P. Lemaitre, E. Sergienko, A. Arnaud, N. Bousquet, F. Gamboa, and B. Iooss. Density modification based reliability sensitivity analysis. *Journal of Statistical Computation and Simulation*, 85:1200–1223, 2015.